Published in final edited form as:
Neuroscience. 2009 December 15; 164(3): 918–928. doi:10.1016/j.neuroscience.2009.08.070.

BASAL AND HYPERCAPNIA-ALTERED CEREBROVASCULAR PERFUSION PREDICT MILD COGNITIVE IMPAIRMENT IN AGING RODENTS: AN MRI STUDY USING FAIR AND BOLD IMAGING

M. Mitschelen[1], **P. Garteiser**[2], **B.A. Carnes**[1], **J. A. Farley**[1], **S. Doblas**[2], **J.H. DeMoe**[2], **J.P. Warrington**[1], **H. Yan**[1], **M.M. Nicolle**[3], **R. Towner**[2], and **W.E. Sonntag**[1,*]

[1]Reynolds Oklahoma Center on Aging, Department of Geriatric Medicine, University of Oklahoma Health Sciences Center, Oklahoma City, OK 73104

[2]Advanced Magnetic Resonance Center, Oklahoma Medical Research Foundation, Oklahoma City, OK 73104

[3]Departments of Internal Medicine and Physiology/Pharmacology, Wake Forest University School of Medicine, Winston-Salem, NC 27157

Abstract

With increasing age, a subset of otherwise healthy individuals undergoes impairments in learning and memory that have been termed mild cognitive impairment (MCI). The enhanced neuronal activity associated with learning and memory requires increased cerebral blood flow (CBF) to specific brain regions. However, the interactions between cerebral blood flow and MCI remain unclear. In this study, we address whether baseline or hypercapnia-induced (increased blood CO_2 levels) changes in CBF are modified with age, and whether these measures are predictive of cognitive status in rodents. Adult and aged rats were evaluated using a hippocampally-dependent task in a water maze. Aged rats were classified as memory-impaired or memory-intact based on performance comparisons with adult rats. Cerebral blood flow was assessed using flow-alternating inversion recovery (FAIR) magnetic resonance imaging (MRI), before and after breathing 10% CO_2. The transition period between CO_2 concentrations was examined with blood oxygen level dependent (BOLD) MRI. Separation of aged animals into memory-intact and impaired categories revealed increased basal perfusion in the dorsal hippocampus of memory-impaired versus memory-intact aged animals. Linear regression revealed that higher hippocampal perfusion was correlated with impaired memory in aged animals, and a logistic regression indicated that hippocampal perfusion predicted spatial memory ability. Several brain regions of aged rats demonstrated an attenuation of the perfusion increase normally observed in adult rats under hypercapnia. Memory-impaired animals were the primary contributor to this effect, as their perfusion response to hypercapnia was significantly reduced compared to adult animals. Aged, memory-intact animals were not significantly different from adults. BOLD MRI demonstrated a reduced response in aged animals to hypercapnia, with impaired animals being the primary contributor to the effect. A logistic regression model based on basal and hypercapnia perfusion correctly predicted cognitive status in 83.3% of animals tested. Our results

*Corresponding Author: Reynolds Oklahoma Center on Aging, University of Oklahoma Health Science Center, 975 NE 10th Street, BRC-1303, Oklahoma City OK 73104, Telephone (405) 271-7622, Fax (405) 271-2298, william-sonntag@ouhsc.edu.

indicate that age-related changes in vascular reactivity and perfusion are important contributing factors in memory impairment.

Keywords

functional imaging; aging; learning; memory

INTRODUCTION

Twenty percent of the population of the United States will be over the age of 65 by 2030 (US Census Bureau, 2004) and studies suggest that as many as 30% of these individuals will develop cognitive impairments ranging from mild cognitive impairment (MCI) to severe dementia associated with pathological diseases such as Alzheimer's Disease (AD). Although MCI is generally considered a transition stage between normal age-related cognitive decline and Alzheimer's Disease, there is a subset of patients with MCI that remain stable and do not progress into dementia (Kelley and Petersen, 2007). The clinical profile of MCI includes deficits in the memory domain that are dependent upon the integrity of the hippocampus/medial temporal lobe.

The flexible use of memory, as required for spatial navigation, is dependent upon the hippocampus and can be reliably measured in rodents (LaSarge and Nicolle, 2009). Spatial learning is impaired after hippocampal lesions in young animals and it also declines reliably with increasing age in both rodents and humans (LaSarge and Nicolle, 2009). Aged rats exhibit individual variability in their spatial learning ability: some animals perform similarly to younger adult animals, while a subset of aged animals perform substantially outside the range of younger rats and are classified as learning impaired (Gallagher, Burwell and Burchinal, 1993; for review see LaSarge and Nicolle, 2009). This 'cognitive aging' is not a result of sensory or motor deficits, but instead reflects individual changes in the biological circuitry necessary to perform a spatial learning task, making it an excellent model of MCI in humans. The Fisher344xBN F1 rat (F344xBN), used in this study, develops spatial learning deficits by 26 months of age and demonstrates a range of spatial learning ability that allows for correlational or predictive analyses based on neurobiological measures.

Although the etiology of MCI remains unknown, a decline in cerebral blood flow or a mismatch between metabolic demand and blood flow have the potential to be important contributing factors in brain aging and the genesis of MCI. Investigators using a variety of imaging methods have reported that cerebral blood flow (CBF) is significantly reduced in aged humans compared to young adults (see, for example, Martin et al., 1991; Moeller et al., 1996; Farkas and Luiten, 2001; Kawamura et al., 1993) and that CBF is correlated with age (e.g.,Krejza et al., 1999; Schultz et al., 1999). Significantly, age-related decreases in CBF appear to be regionally distinct (Martin et al., 1991; Moeller et al., 1996; Bentourkia et al., 2000; Hagstadius and Risberg, 1989; Pagani et al., 2002) and may begin as early as middle age (Schultz et al., 1999) or even teenage years (Biagi et al., 2007) in humans. Furthermore, differences in regional CBF have been reported to discern frontotemporal dementia from Alzheimer's Disease (Du et al., 2006), predict conversion from mild cognitive impairment to AD (Wang et al., 2009), and exist in both depressed AD patients and patients with vascular dementia (Kato et al., 2008; Levy-Cooperman et al., 2008; Dai et al., 2009).

Perfusion imaging by nuclear magnetic resonance is an invaluable tool for the collection of *in vivo* data on the functional state of the cerebral vasculature. Although positron emission tomography (PET) (Ito et al., 2002) or single photon emission computed tomography (SPECT) (Kato et al., 2008) can be used to assess the effects of aging and dementia on cerebral perfusion

rates in humans, the limited resolution of these techniques renders them less capable of resolving regional CBF differences in rodent studies. Conversely, high field magnetic resonance imaging (MRI) of small animals allows greater resolutions to be achieved without involving radiolabeled injectable tracer compounds. Blood perfusion measurements by MRI traditionally involve either flow-sensitive alternating inversion recovery (FAIR) or arterial spin labeling (ASL) techniques. Because ASL uses a small coil positioned at the carotid artery to generate a small bolus of blood with inverted spins, interpretation of ASL results is complicated by anastomotic perfusion and diffusion phenomena, which tend to distribute the tagged bolus temporally and spatially (Gallichan and Jezzard, 2009). Furthermore, it was recently shown that FAIR compares favorably to ASL techniques at high field with respect to labeling profile and static signal suppression, resulting in improved sensitivity of perfusion maps, better signal-to-noise ratio, and quality of the magnetization regrowth fitting procedures (Gardener, Gowland and Francis, 2009), making it particularly useful for examination of regional CBF changes in aged rats.

In the present study we use hypercapnia (increased blood CO_2 levels) as a stimulus to probe the responsiveness of the vasculature in relationship to age and spatial learning ability. We use hypercapnia to maximally increase cerebrovascular perfusion in anesthetized animals in the absence of behavioral or tactile stimuli (see, e.g., Sicard and Duong, 2005). To measure these responses, we utilize FAIR, to assay perfusion, and blood oxygen level dependent (BOLD) fMRI, to observe transient changes in local oxyhemoglobin levels. We demonstrate regional CBF differences between aged and younger adult animals, and between memory-impaired and memory-intact aged animals. Our results indicate that basal hippocampal perfusion and vascular reactivity in multiple brain regions (e.g. response to hypercapnia) are highly predictive of spatial learning ability in aged rats and can distinguish aged rats with preserved cognitive function from those with impairment.

METHODS

Theory in Brief

FAIR MRI (Kim, 1995) images total water flow through a slice of interest by inverting proton spins in the slice (slice-selective; SS), and comparing the spin relaxation rate to the relaxation rate observed when inverting proton spins in the entire head (global, or non-selective; NS). During a SS inversion, protons with an inverted spin can move out of the slice, but protons moving into the slice will be relaxed, as their spins have not been inverted. During a NS inversion, the apparent relaxation rate in the slice of interest will closely reflect the natural relaxation rate for the tissue – water protons moving in and out of the slice will have had their spins inverted. In this manner, the apparent relaxation rate for a SS inversion is increased – inverted proton spins are both relaxing at their natural rate *and* being replaced by non-inverted protons from outside the slice. Therefore, to having meaningful perfusion data, there must be a significantly higher spin relaxation rate observed during SS inversions than in NS inversions. If this is not the case, measured perfusion rates are too greatly masked by noise to be considered meaningful.

BOLD MRI images local changes in oxyhemoglobin levels by virtue of the increased spin relaxation rate of a high deoxyhemoglobin environment compared to a high oxyhemoglobin environment. As a result, the signal decreases with higher tissue metabolism of oxygen, but increases with the perfusion of oxygenated arterial blood (Hoge et al, 1999). In the case of hypercapnia, which is considered isometabolic (Bulte, Drescher and Jezzard, 2009), the primary contributor to the BOLD signal would be changes in arterial blood perfusion. Pixels with positive correlation to the stimulus reported in this study are pixels with increasing oxyhemoglobin levels. In this study, we use BOLD and FAIR in concert to provide further

confirmation that observations are based upon cerebrovascular perfusion rather than possible confounding factors.

Animals

Male Fisher 344 x Brown Norway F1 rats were purchased from the National Institute on Aging breeding colony at Harlan Industries (Indianapolis, IN). Animals were singly housed in a specific pathogen-free rodent barrier facility at The University of Oklahoma Health Science Center (OUHSC) in laminar flow caging on a 12h light / 12h dark cycle, and given standard rodent chow (Purina Mills, Richmond, IN) and water *ad libitum.* Rats were adult (9.5 months, n=6) or aged (26 months, n=14) at the time of behavioral analysis. After completion of behavioral testing, animals were transferred to the Oklahoma Medical Research Foundation (OMRF) and housed under the same conditions for one week before initiating MRI studies. The animals were either 12 or 28.5 months old at the completion of the MRI studies. Two aged animals were not included in the MRI analyses, as one had a pituitary tumor and the other died during imaging. All animal protocols were approved by the Institutional Animal Care and Use Committees of OUHSC or OMRF.

Behavioral Analysis

Spatial memory was assessed using a Morris water maze as previously described (Gallagher, Burwell and Burchinal, 1993; LaSarge and Nicolle, 2009). Briefly, the maze was 175cm in diameter with water 40cm deep and made opaque with non-toxic white paint. Curtains surrounded the maze and visual cues were placed at several locations. A retractable escape platform was available during the acquisition trials, hidden 2cm below the surface of the water. For eight consecutive days, animals were allowed 3 trials of 90s each. Those animals that failed to find the platform in 90s were guided to it by the investigator. Once on the platform, rats were allowed 15s to acquire memory of its position. Every sixth trial (the third trial every second day) was a probe trial, where the platform was lowered to an unavailable position for the first 30s, and raised for the final 60s of the trial. The mean proximity of animals to the platform was sampled over 28s while the platform was unavailable. This measurement, using EthoVision XT 5 software (Noldus, Wageningen, Netherlands), averaged across 3 probe trials for each rat, was used as a score of the animal's cognitive ability. The proximity measure in a water maze has been reported to be more sensitive than either path length or latency measures in aged animals (Gallagher, Burwell and Burchinal, 1993). During training (non-probe) trials, the length of the path the animal followed to the platform was measured. In cases where animals did not find the platform, total path length recorded was the total distance traveled over the 90s. Swim velocities were also analyzed. Three (3) days after completing this task, rats were tested in the maze with a visible (raised) platform to verify that performance deficits were not due to poor vision or motor impairment. Visible platform training consisted of 4 trials in one day with cues around the maze removed.

Hypercapnia for MRI

Animals were initially anesthetized with isoflurane (2.0–2.5%) in the carrier gas and immobilized in the imaging cradle. Subsequently the isoflurane was reduced to 1.5–2% in an effort to decrease the anesthesia-induced dampening of the perfusion response (Sicard et al., 2003). Preliminary studies with an independent cohort of animals used oxygen as a carrier gas, but MRI analysis failed to discriminate between groups, and air was used in all subsequent studies. During the initial period of anesthesia, reference images were taken and localized field shimming was performed. An imaging scan was taken while the animals were in this basal state to provide a baseline value for perfusion rates. At the end of the baseline perfusion imaging BOLD (T_2*-weighted dynamic) acquisition was initiated, after which the carrier gas was switched to 10% CO_2 in 90% carrier gas on a volume basis. The animals were allowed to

acclimate to the CO_2-enriched gas for an additional 12 minutes during which the T_2*-weighted dynamic acquisition was continued. After the acclimation period, a second perfusion imaging dataset was acquired to provide data in the hypercapnia state.

MRI- reference images

High-resolution images for morphological reference were acquired prior to hypercapnia-related acquisitions. The rapid acquisition, relaxation-enhanced (RARE) pulse sequence was used with a repetition time of 3000ms, an echo time of 17ms and a RARE factor of 8, for a total scan time of 5min. The geometries used were the same as the geometries of the perfusion and BOLD acquisitions, but with isometric in-plane resolutions of 200μm for perfusion and 312μm for BOLD images.

MRI- FAIR

Perfusion maps were obtained on a single coronal slice of the brain (as defined according to the stereotaxic reference frame of Paxinos and Watson, 2007) set to intersect the dorsal hippocampus with a maximal cross-section. The imaging geometry was a 25.6mm × 25.6mm slice 2.0mm thick. The cerebral perfusion contrast was obtained using the flow-sensitive alternating inversion recovery (FAIR) acquisition strategy (Kim, 1995). Briefly, two series of inversion recovery images were acquired using 4 inversion recovery times evenly spaced from 20ms to 2420ms. The acquisition scheme was a single shot echo-planar encoding over a 64×64 matrix using an echo time of 20ms. The first series (slice-selective; SS) was acquired by applying the inversion pulse to a 6mm section overlapping and centered on the imaging slab. The 2mm margins on either side of the imaging slice were implemented in an effort to reduce the influence of the non-ideal properties of the gradients and RF pulse used for slice selection. The second series (non-selective; NS) was acquired by applying a non-spatially restricted inversion pulse. A repetition time of 18s was adopted in an effort to minimize artifacts due to recirculation of inverted spins inside the slice of interest (this is discussed briefly in Gallichan and Jezzard, 2009). It is known that variations in oxygenation levels between acquisition of the SS and NS images may complicate the interpretation and decrease the sensitivity of FAIR results (Lu, Donahue and van Zijl, 2006). In our study, these effects were minimized by implementing acclimation periods that were long compared to the characteristic interleaving time of the pulse sequences that were used.

MRI- T_2*-weighted imaging

BOLD imaging was implemented by acquiring echo-planar imaging with T_2* contrast. An echo-planar imaging sequence was used with a repetition time of 2000ms, an echo time of 22ms, a flip angle of 30° and 4 excitations per slice. The geometry consisted of 8 contiguous horizontal slices (as defined according to the stereotaxic reference frame of Paxinos and Watson, 2007) 1.2mm thick and 40mm square. Each slice was encoded over a 64×64 matrix. The temporal resolution using this acquisition scheme was 8s. 150 such repetitions were acquired, and the reaction of the animal to the increase in CO_2 content was captured from the 60^{th} repetition to the end of the acquisition.

Data processing

For FAIR analysis, the recovery curves obtained from each pixel of the global (S_{NS} (TI) = $A - B \cdot e^{-TI/\tau NS}$) or selective ($S_{SS}$ (TI) = $A - B \cdot e^{-TI/\tau SS}$) inversion images were numerically fitted to derive the pixelwise τ_{NS} and τ_{SS} values, respectively. In these expressions, A and B are constants, TI is the operator-controlled inversion time, and the apparent longitudinal recovery rates ($1/\tau_{NS}$ and $1/\tau_{SS}$) are introduced as

$1/\tau_{NS}=(1/T_1)+(T_E/T_1 \cdot T_2^*)$ and, $1/\tau_{SS}=(1/T_1)+(T_E/T_1 \cdot T_2)+(f/\lambda)=(1/\tau_{NS})+(f/\lambda)$

respectively. These longitudinal recovery rates were then used to calculate the perfusion rate,

f (ml/(100g·s)) on a pixelwise basis using the relationship $f=\lambda\cdot(1/\tau_{NS}-1/\tau_{SS})$, thereby canceling out possible confounds from tissue T_1 and T_2^*. Regions of interest (ROIs) were manually outlined around the whole cross-section of the brain, the cortex, the dorsal hippocampus, the retrosplenial cortex and the thalamus using the global inversion images obtained at an inversion time of 2420ms, and a rat brain atlas (Paxinos and Watson, 2007). The areas overlapping large blood vessels were filtered by discarding any pixels with abnormally high or low values (outside of an interval of 0 to 150 ($ml_{blood}/(g_{brain}\cdot s)$)). Less than 5% of the pixels of any ROIs were removed by this filtering step.

For BOLD imaging analysis, the evolution of pixel intensity over time was analyzed by evaluating its correlation to the hypercapnia stimulation paradigm, which was modeled as a step function with offset at frame 70. Although CO_2 was present in the anesthesia during frame 60, frames 60 to 70 were discarded to account for the dead volume of the tubing (17.66s or 1.1 frame assuming plug flow) and the remaining 8.9 frames were discarded to account for potential gas mixing. These data were used to create a multislice map of correlation coefficients (r) ranging from 0 to 1. For the purpose of methods comparisons, those voxels located at anatomical coordinates outside of the field of view used in FAIR perfusion imaging were cropped out of further analyses, although entire slices were still stored for display. Pixels with correlation coefficients comprised between $r= 0.6$ and $r= 0.8$ were counted, and this number was expressed as a percent of the total number of pixels in the corresponding coronal section of the brain. The resulting values were used for statistical analysis.

Blood sampling

Before MRI, the inner leg and abdomen of the animals were shaven for post-imaging blood sampling. Once the MRI procedure was completed, rats were transferred to a heated pad and maintained on the same gas mixture used at the end of the imaging session (10% CO_2 in air, as a carrier gas for isoflurane). After positioning for surgery, the inner leg and abdomen were swabbed with iodine (Vedco, St. Joseph, MO). The left femoral artery was exposed by blunt dissection, and isolated from the adjacent vein and nerve. The artery was clamped both distally and proximally with micro vascular clips to temporarily achieve hemostasis, and the vessel was then catheterized using a 24ga Insyte™ Autogaurd™ (Becton-Dickinson, New Jersey). One ml of arterial blood was drawn and analyzed using an i-STAT® clinical analyzer (Heska, Loveland, CO). Blood analyte results are reported normalized to 37°C by the analyzer. The vessel was cauterized and the wound was closed with silk suture and tissue adhesive. For post-operative hydration, animals were given 3ml saline subcutaneously and 40mg cefazolin (Westward, Eatontown, NJ) was administered intramuscularly to prevent infection. One animal died during surgery, and several blood analyte cartridges failed, resulting in different sample numbers for blood analytes and MRI data.

Statistical analysis

Water maze training trial data were analyzed with a repeated measures ANOVA (block × age or block × behavioral group), using Statview (SAS Institute, Cary, NC). All other data were entered into Sigma-Stat 3.5 (Systat Software, Chicago) for analysis. Data grouped by age were analyzed with Student's t-test (or Mann-Whitney U, for non-parametric data), and data by behavioral group were analyzed by ANOVA. Significant interactions were further examined by Bonferonni post-hoc t-tests. Linear regression p-values are derived from regression model summaries comparing the contributions to variance from the expected regression values versus randomness in the sample, and r^2 values are presented unadjusted. Results are presented as mean ± SEM.

Subsequently, logistic regression (using SAS, 2008 Cary, NC) was used to predict the probability (p_i) that a particular animal was impaired (binary response variable, IMP = 1) or not (IMP = 0):

$$\text{logit}(p_i)=\log[p_i/(1-p_i)]=\sum \beta_i x_i$$

where β_i are logistic regression coefficients, x_i are predictor variables (*i.e.*, an intercept plus 13 measurements derived from MRI data), $p_i/(1-p_i)$ is the odds ratio, and $\log[p_i/(1-p_i)]$ is the log odds ratio or logit (SAS Institute Inc., 1995). Mean proximity to platform (cm) was used to create a response variable for the logistic regression under the assumption that proximity is correlated with degree of cognitive impairment. Three partitions of proximity scores into intact/impaired subgroups were considered with 4, 5, or 6 animals in the impaired group.

All 13 predictor variables (absolute and relative perfusion measurements from all ROIs, and BOLD results) were included in the initial logistic model, and a final model was achieved by the progressive backwards elimination of non-significant variables with 0.15 used as the significance level required for retaining variables in the model. Model performance was assessed by the maximum likelihood ratio statistic (LRS), area under the Receiver Operating Characteristic (ROC) curve (c statistic), and the resulting sensitivity (correct identification of impaired animals) and specificity (avoiding false negatives and false positives) of the assignments to intact/impaired groups, using assignment thresholds that reflected the approximate observed distribution of intact/impaired in the data analyzed.

RESULTS

Assessment of Spatial Learning Ability

Adult and aged rats both acquired the spatial learning task, indicated by a main effect of training block and significantly shorter path lengths required to find the platform location over the course of training ($p< 0.0001$; Fig. 1a). Overall, however, the aged rats had less proficient spatial learning ability than the adult rats, indicated by an interaction between age and trial block ($p= .037$). Subsequent unpaired t-tests showed a trend towards poorer performance of the aged rats on training block 2 ($p= .08$). In training block one there was a significant effect of age on swim velocity ($p< 0.001$). This contributed to the moderately shorter path length for aged animals in block one seen in Fig. 1a, though this difference was insignificant. Visible platform training confirmed that there were no significant differences in swim speed between adult and aged rats when considering all trials together ($p= 0.639$, data not shown). Therefore, the poorer performance of the aged rats can be attributed to cognitive dysfunction and not sensorimotor deficits.

The poorer spatial learning ability by the aged group is reflected in the probe trial data, with the aged rats having a less accurate search for the escape platform location compared to the adult group ($p= 0.007$; Fig. 1c). The individual variability in spatial learning ability shown in Fig. 1c was exploited to define aged rats with impaired or relatively preserved memory compared to the adult group. Aged rats were categorized into “intact” and “impaired” groups using a probe trial proximity score corresponding to the 66.67 percentile of rats with a complete (including MRI) data set. This was equivalent to 2.86 SDs greater than the mean proximity score for adult animals ($n= 6$); (Aged: $n_{intact}= 8$, $n_{impaired}= 6$ for behavioral data). As shown in Fig. 1d, these behavioral groupings create an aged intact group with equivalent performance to the adult group and an aged impaired group with significantly poorer performance than either the adult group ($p< 0.001$) or aged intact group ($p< 0.001$). Acquisition data was re-analyzed based on behavioral group comparisons to determine if the aged spatial learning-impaired

group could be distinguished from the adult and aged-intact rats. Fig. 1b illustrates the overall poorer performance of the spatial learning-impaired rats compared to the aged-intact and adult rats. A nearly significant group effect ($p= 0.055$) existed when aged rats were categorized as intact or impaired, and this was primarily due to the significant difference between aged intact and impaired animals (Fisher's PLSD, $p= 0.02$). Examining block 3 individually, there is a distinct difference between the aged impaired and intact animals ($p= 0.018$), and between the aged impaired and adult animals ($p= 0.022$). Therefore, aged impaired animals were the primary contributor to the difference observed between aged and adult rats during training trial acquisition.

Validation of FAIR MRI

In agreement with the assumptions of our study, longitudinal relaxation rates derived by numerical fit were higher after SS inversions than NS inversions in all situations, irrespective of hypercapnia or age (Table 1). Under hypercapnia, SS and NS longitudinal relaxation rates increased in both age groups ($p< 0.0001$ for adult SS, adult NS, aged SS, and aged NS R_1 increases under hypercapnia). Therefore, our perfusion calculations are entirely dependent upon perfusion, without possible confounds from changes in oxygen level (see *Blood Analysis*).

FAIR MRI

Baseline perfusion did not differ significantly by age (Fig. 2a) when air was used as the carrier gas. However, when separated into intact and impaired categories, aged impaired animals had a significantly higher baseline perfusion in dorsal hippocampus than aged intact animals ($p= 0.045$, Fig. 2b). Higher baseline hippocampal perfusion was associated with poorer individual cognitive performance in older animals (linear regression $r^2= 0.54$, $p= 0.006$, Fig. 6a). Furthermore, baseline perfusion of dorsal hippocampus was the only measure (from FAIR and BOLD analysis) that survived a reverse stepwise logistic regression designed to predict whether an aged animal was impaired or intact when classified as above (see *Predictors of Cognitive Ability* below).

Perfusion responses to hypercapnia differed significantly by age and cognitive ability (Fig. 3). Older animals showed lower perfusion increases in response to hypercapnia in the whole brain crossection ($p= 0.004$), cortex ($p= 0.017$), and thalamus ($p= 0.036$) when compared to adult animals (Fig. 3a). When separated by cognitive status, aged impaired animals exhibited an attenuated increase in perfusion in response to hypercapnia in whole brain ($p= 0.014$) and thalamus ($p= 0.025$) compared to adult animals, but no significant differences were found between aged intact and adult animals, nor between aged impaired and aged intact animals (Fig. 3b).

The different brain regions that were examined responded to the hypercapnic challenge with perfusion increases of varying magnitude, but no statistical differences were found between any two regions of interest. The retrosplenial cortex was the region with the highest percent change in perfusion under hypercapnia in both age groups, although the high variability associated with this region prevented it from reaching statistical significance. A similar response could also be seen in the corresponding perfusion increase in cortex (see perfusion maps, Fig. 4). No increase in perfusion rate in response to hypercapnia could be found when using pure oxygen as the carrier gas in any of the age groups (data not shown).

BOLD MRI

Voxels from BOLD images of each animal that intersected with their FAIR voxels were examined for their response to hypercapnia (Fig. 5). Aged animals showed a significantly lower percentage of voxels within thresholds (see Methods) than did adult animals ($p= 0.004$, Fig.

5a). Similar to the data obtained by FAIR analysis, BOLD MRI indicated that aged impaired animals exhibited a significantly lower percentage of voxels within thresholds than adult animals ($p= 0.03$), but were not significantly different from aged intact animals, nor were aged intact animals significantly different from adult animals (Fig. 5b).

Blood Analysis

Arterial blood from animals under hypercapnia showed no significant differences between age groups, or when older animals were categorized by performance in the water maze, for Na^+, K^+, ionic Ca^{2+}, hematocrit, or hemoglobin, nor did these values differ from accepted normal ranges. Neither pH nor pO_2 were significantly different when compared by age or maze performance, but were low across all animals (pH 6.912 ± 0.018; pO_2 70.9 ± 5.1 mmHg), as may be expected after prolonged hypercapnia. pCO_2 levels for all animals were greater than 130 mmHg during the hypercapnia stage of the study.

Predictors of Cognitive Ability

In addition to the association between hippocampal perfusion and performance on tests of learning and memory observed in aged animals (see above), other measurements were correlated with learning and memory in our cohort. Linear regressions indicated that higher baseline perfusion of the whole brain crossection ($r^2= 0.295$, $p= 0.020$) and reduced perfusion increases in response to hypercapnia ($r^2= 0.299$, $p= 0.019$) corresponded with poorer cognitive performance in the water maze. Calculation of a perfusion index ([baseline perfusion] / [ratio of hypercapnia perfusion to baseline perfusion]) for the whole brain crossection correlated strongly to cognitive performance (linear regression $r^2= 0.432$, $p= 0.003$, Fig. 6b). Furthermore, linear regression using this index conformed to assumptions of constant variance and normality. Similarly, baseline and hypercapnia perfusion responses in the thalamus were associated with cognitive performance (baseline $r^2= 0.299$, $p= 0.019$; response $r^2= 0.296$, $p= 0.020$). While a thalamic perfusion index of our cohort was not normally distributed, it also was a strong correlate of cognitive ability ($r^2= 0.401$, $p= 0.005$, data not shown).

Further examination of aged animals alone using a reverse stepwise logistic regression yielded no predictor variables that survived backwards elimination when using 6 animals in each category (separated at the 50^{th} percentile in water maze performance). When 5 animals were assigned to the impaired category (separated at the 58.3 percentile), the whole brain perfusion index ($p= 0.10$) and cortical baseline perfusion ($p= 0.14$) were retained in the final model (LRS = 0.03; c = 0.914; sensitivity = 0.80, specificity = 0.86, Mantel-Haenszel χ^2 $p= 0.029$). The relationship between baseline cortical perfusion and behavioral performance did not reach statistical significance by linear regression ($p= 0.087$), but does contribute significantly to the predictive value of the logistic regression model. When 4 animals were assigned to the impaired category (separated at the 66.67 percentile, as in analyses above), dorsal hippocampal perfusion ($p= 0.14$) was the sole predictor variable retained in the final logistic model (LRS = 0.02; c = 0.83; sensitivity = 0.75, specificity = 0.75, Mantel-Haenszel $\chi^2 = 2.51$, $p= 0.11$).

DISCUSSION

In this study we demonstrate that impairment of hippocampally-dependent spatial memory in aging rats is associated with an increased basal CBF in dorsal hippocampus, and reduced perfusion responses to hypercapnia across the brain, particularly in cortex and thalamus. A similar reduction in response to hypercapnia in memory-impaired rats was confirmed using BOLD imaging. Furthermore, these physiological impairments were not evident in aged rats with intact spatial memory. While the division of aged animals into “intact” and “impaired” categories is, by nature, relative, our analyses revealed that alterations in regional blood flow were highly predictive of learning and memory performance. Analysis of baseline perfusion

under normal blood CO_2 levels (normocapnia) not only indicated physiological similarities between aged intact and adult animals, but revealed differences between aged intact and impaired animals. Importantly, the only significant difference between normocapnic aged impaired and unimpaired animals was basal perfusion in the dorsal hippocampus. These results are in qualitative agreement with numerous studies of several dementias and mild cognitive impairment in humans, where differences in CBF between healthy and impaired patients were isolated to specific brain regions dependent upon the specific type of deficit (Du et al., 2006; Wang et al., 2009; Kato et al., 2008; Levy-Cooperman et al., 2008). The fact that the differences in basal perfusion were detectable only in hippocampus suggests that this brain region exhibits relatively unique changes in blood flow that correlate closely with mild/moderate impairments in learning and memory, and that these differences can be revealed by non-invasive, high-resolution perfusion imaging techniques.

Although the etiology for the increases in basal hippocampal perfusion in aged cognitively impaired animals are unknown, we have previously proposed that age-related changes within the vasculature could contribute significantly to diminished tissue function by creating a condition of chronic mild hypoxia. As hypoxia-induced angiogenesis is impaired with age in the hippocampus of F344xBN rats (Ingraham et al., 2008), this hypothetical state is unlikely to be self-correcting, and quite possibly would enter a vicious cycle of increasing hypoxia in the hippocampus. In earlier studies, we reported an age-related decline in pre-capillary arteriolar density in F344xBN rats using a cranial window approach (Sonntag et al., 1997) while few changes were evident in capillary density (Ingraham et al., 2008). These studies have led to the conclusion that pre-capillary arterioles may be highly sensitive to the effects of age – either through impairments in response to acute metabolic stimuli (e.g. elevated CO_2 levels), through vessel rarefaction, or both. We propose that the increased basal perfusion rate in hippocampus of the aged impaired animals observed in this study is, paradoxically, due to the *decline* in pre-capillary arterioles, which results in increased dilation of the remaining vessels. Increasing perfusion only enough to restore it to levels observed in healthy hippocampus would be insufficient, as there is a reduction in the number of vessels bringing oxygenated blood. This places tissue farther downstream of oxygenated blood, reducing the efficiency of oxygen transfer by loss of blood oxygen to upstream tissues. Increased basal perfusion through a reduced pre-capillary arteriole network would limit the amount of further perfusion increases possible, partially explaining the general reduction in hypercapnia response observed in aged impaired animals. Though this effect did not reach statistical significance in the dorsal hippocampus, it was the region with the greatest reduction in hypercapnia response in aged impaired animals. Because increased neuronal activity (and therefore, learning and memory) are dependent upon an acute increase in perfusion, impairments in vascular function are likely to be important factors that result in neuronal dysfunction. Together with previously published data, this study provides compelling data that arteriolar rarefaction and/or impairments in vasodilatory responses to metabolic stimuli (e.g., hypercapnia) are contributing factors in the development of mild cognitive impairment.

Previous perfusion studies in rodents have shown that the response to hypercapnia is dose- (Sicard and Duong, 2005), region- (Lu et al., 2009), and strain-dependent (Takahashi et al., 1996). In this study, we used 10% CO_2 with room air as the carrier gas, which has been demonstrated to create a nearly maximal increase in CBF (Sicard and Duong, 2005). Consistent with a previous study in Sprague-Dawley rats (Takahashi et al., 1996), the F334xBN strain used in this study exhibited a higher response to hypercapnia in cortex than subcortical regions (Fig. 3). However, significant differences between aged impaired and adult rats in our study were found in the thalamus as well as the whole brain crossection, and these regions exhibited a significant correlation with hippocampally-dependent maze performance. Though the correlation between cognitive performance and thalamic perfusion is unexpected, it appears reasonable that the effects of aging on the vasculature would not be limited to the hippocampus,

and, in fact, may be more apparent in the largest regions examined due to the higher number of pixels sampled. Our examination with BOLD imaging of the transition from normocapnic to hypercapnic conditions showed a similar attenuation of the hypercapnia response across the brain in aged impaired animals when compared to adult animals. Thus, while either technique is capable of discerning differences between groups, the robustness of these findings in other species or strains requires further studies.

Beyond demonstrating differences between groups divided by cognitive status, FAIR perfusion imaging provided data predictive of individual cognitive ability. Hippocampal perfusion, whole brain crossection and thalamic baseline perfusion, as well as their respective hypercapnia responses, demonstrated significant correlations to water maze performance in individuals from all groups. As a result, a perfusion index (combined baseline perfusion and response to hypercapnia) for each of these regions was created. These measures demonstrated extremely strong ($p< 0.005$) correlations to water maze performance. Furthermore, the whole brain crossection index was one of two measures that remained in a more stringent logistic regression model designed to assess predictors of learning and memory performance. That we could create a predictive model with 80% sensitivity and 86% specificity using data from only 12 aged animals suggests the importance of CBF for healthy memory acquisition and retention. The less stringent model (using the same division of aged animals described elsewhere in this study) performed slightly worse (75% sensitivity and specificity), and pointed to dorsal hippocampus baseline perfusion as the only significant predictor of cognitive status, consistent with the hippocampal dependence of our memory test. It is not surprising that the two models use different predictor variables, as one is designed to be more sensitive to slight memory impairments and the other is designed to find animals only with more significant deficits. The reverse stepwise procedure used in our study discards any variables that fail to increase the predictive value of the model. Therefore, exclusion from the model is not indicative of a lack of correlation, but only a failure to improve the predictive value beyond what is possible with the variables meeting retention criteria.

It has been reported on several occasions that, somewhat paradoxically, tissue oxygen levels may increase under hypercapnia. It is possible that the effect of the paramagnetism of O_2 increasing the longitudinal relaxation rates ($1/\tau$) (Janne d'Othee et al., 2003; Zaharchuk et al., 2005) may have dominated the T_1 term in the expressions for $1/\tau$. However, we observed generally hypoxic pO_2s under hypercapnia with air as a carrier gas. If instead the T_2* term were predominant, then the opposite trend would be observed, whereby $1/\tau$ values would decrease under hypercapnia. It is possible that under our experimental conditions, where hypercapnia was maintained for an extended period of time (26 minutes at the end of imaging), we may have elicited a state where the Bohr effect becomes predominant, and where the $1/\tau$ values are dominated by the T_2* term. This hypothetical state would be accompanied by a depletion of oxygen from the hemoglobin pool, resulting in the increased apparent longitudinal relaxation rates that we measured. Furthermore, preliminary studies using pure oxygen as a carrier gas failed to elicit statistically detectable perfusion changes. Diminished perfusion responses to hypercapnia using oxygen as a carrier gas has also been observed in humans (Bulte, Drescher and Jezzard, 2009). One could argue that by increasing perfusion and by reducing metabolism, the animals could compensate for the decreased oxygen content of arterial blood. However, there was no perfusion increase in aged animals, despite having higher $1/\tau$ values under hypercapnia. Furthermore, hypercapnia is generally considered isometabolic (Bulte, Drescher and Jezzard, 2009). Based on these considerations, the apparent longitudinal relaxation rates that were required for calculating FAIR perfusion maps are insufficient to determine tissue pO2 levels under hypercapnia in the various age groups in the absence of separately determined $1/T_2$* and $1/T_1$ values. Approaches such as those used in calibrated fMRI (Davis et al., 1998; Hoge et al., 1999) may prove beneficial in addressing this particular aspect. Nevertheless, our FAIR perfusion results could not be an artifact of tissue oxygen level

differences between groups because of the cancellation of pO2-sensitive terms in the expression for the perfusion.

While it is possible to perform perfusion MRI in unanaesthetized rats to avoid the dampening effect of anesthesia on CBF response to hypercapnia (Sicard et al., 2003), this comes with technical challenges and at the cost of animal discomfort and stress that may differentially affect CBF. The Sicard *et al.* study (Sicard et al., 2003) used pulsed arterial spin labeling (ASL) in a 4.7T field. However in our study, FAIR was used with a field strength of 7T. Sensitivity is generally higher at higher field strengths, and FAIR has been proposed as more sensitive than ASL (Gardener, Gowland and Francis, 2009). This may have contributed to our ability to observe perfusion response differences between cognitive groups, despite the deleterious effects of anesthesia.

Although the sensitivity of the FAIR imaging was sufficient to discern physiological differences in animals with different memory abilities, significant improvements may be possible. In particular, there may exist a series of inversion times (TIs) whose sampling may result in a better signal-to-noise ratio. Our choices of TIs were, however, sufficient to provide a significantly higher relaxation rate following the SS inversion compared to the NS inversion (Table 1) regardless of the age group or inhaled gas. Our BOLD analysis might be improved as well, as it relied on a single transition from normocapnia to hypercapnia, rather than on repeated stimuli generally used in fMRI experiments. Repeated stimuli greatly increased risk of death in the older animals, but it is possible that a reduced hypercapnic challenge may allow such repetition. Furthermore, as only CBF measures were found to have a strong correlation to cognitive ability, it may be reasonable to perform only FAIR analysis. Correlations between blood analytes and cognitive ability were not observed in this study, suggesting that blood sampling may not be necessary once a protocol is established. Without the requirement of any invasive procedure, the potential exists to use these methods in a longitudinal study of aging animals. Finally, consideration of partial volume effects may increase the accuracy of our perfusion measurements in aging rats as it does in aging humans (Asllani et al., 2009).

In conclusion, we have demonstrated that sufficient methods are available to assess cerebrovascular perfusion changes in the aging rat, and that basal perfusion and changes in perfusion in response to a physiological stimulus (hypercapnia) are closely associated with impairments in learning and memory. As similar regional perfusion deficits have been observed in human patients with various dementias and cognitive impairments, our results demonstrate that the rodent is an excellent model for assessing cognitive decline with age, and that interventions targeting the cerebrovasculature may be a potential source of treatment to prevent age-related cognitive decline. The techniques and animal model described in this study may prove a valuable means of assessing such interventions.

Supplementary Material

Refer to Web version on PubMed Central for supplementary material.

Abbreviations

AD, Alzheimer’s disease
ASL, arterial spin labeling
BOLD, blood-oxygen-level-dependent
CBF, cerebral blood flow
F344xBN, Fisher344 x Brown Norway F1
fMRI, functional magnetic resonance imaging
LRS, likelihood ratio statistic

MCI, mild cognitive impairment
MRI, magnetic resonance imaging
NS, non-selective
PET, positron emission tomography
PLSD, protected least significant difference
RARE, rapid acquisition relaxation-enhanced
ROC, receiver operating characteristic
ROI, region of interest
SS, slice-selective
SPECT, single photon emission computed tomography
TI, time of inversion

Acknowledgments

This study was supported by NIA Grant P01 AG11370 and the Donald W. Reynolds Foundation.

REFERENCES

Asllani I, Habeck C, Borogovac A, Brown TR, Brickman AM, Stern Y. Separating function from structure in perfusion imaging of the aging brain. Hum Brain Mapp 2009;9999NA

Bentourkia M, Bol A, Ivanoiu A, Labar D, Sibomana M, Coppens A, Michel C, Cosnard G, De Volder AG. Comparison of regional cerebral blood flow and glucose metabolism in the normal brain: Effect of aging. J Neurol Sci 2000;181:19–28. [PubMed: 11099707]

Biagi L, Abbruzzese A, Bianchi MC, Alsop DC, Del Guerra A, Tosetti M. Age dependence of cerebral perfusion assessed by magnetic resonance continuous arterial spin labeling. J Magn Reson Imaging 2007;25:696–702. [PubMed: 17279531]

Bulte DP, Drescher K, Jezzard P. Comparison of hypercapnia-based calibration techniques for measurement of cerebral oxygen metabolism with MRI. Magn Reson Med 2009;61:391–398. [PubMed: 19165902]

Dai W, Lopez OL, Carmichael OT, Becker JT, Kuller LH, Gach HM. Mild cognitive impairment and alzheimer disease: Patterns of altered cerebral blood flow at MR imaging. Radiology 2009;250:856–866. [PubMed: 19164119]

Davis TL, Kwong KK, Weisskoff RM, Rosen BR. Calibrated functional MRI: Mapping the dynamics of oxidative metabolism. Proc Natl Acad Sci U S A 1998;95:1834–1839. [PubMed: 9465103]

Du AT, Jahng GH, Hayasaka S, Kramer JH, Rosen HJ, Gorno-Tempini ML, Rankin KP, Miller BL, Weiner MW, Schuff N. Hypoperfusion in frontotemporal dementia and alzheimer disease by arterial spin labeling MRI. Neurology 2006;67:1215–1220. [PubMed: 17030755]

Farkas E, Luiten PG. Cerebral microvascular pathology in aging and alzheimer's disease. Prog Neurobiol 2001;64:575–611. [PubMed: 11311463]

Gallagher M, Burwell R, Burchinal M. Severity of spatial learning impairment in aging: Development of a learning index for performance in the morris water maze. Behav Neurosci 1993;107:618–626. [PubMed: 8397866]

Gallichan D, Jezzard P. Variation in the shape of pulsed arterial spin labeling kinetic curves across the healthy human brain and its implications for CBF quantification. Magn Reson Med 2009;61:686–695. [PubMed: 19132757]

Gardener AG, Gowland PA, Francis ST. Implementation of quantitative perfusion imaging using pulsed arterial spin labeling at ultra-high field. Magn Reson Med 2009;61:874–882. [PubMed: 19189295]

Hagstadius S, Risberg J. Regional cerebral blood flow characteristics and variations with age in resting normal subjects. Brain Cogn 1989;10:28–43. [PubMed: 2713143]

Hoge RD, Atkinson J, Gill B, Crelier GR, Marrett S, Pike GB. Investigation of BOLD signal dependence on cerebral blood flow and oxygen consumption: The deoxyhemoglobin dilution model. Magn Reson Med 1999;42:849–863. [PubMed: 10542343]

Ingraham JP, Forbes ME, Riddle DR, Sonntag WE. Aging reduces hypoxia-induced microvascular growth in the rodent hippocampus. J Gerontol A Biol Sci Med Sci 2008;63:12–20. [PubMed: 18245756]

Ito H, Kanno I, Ibaraki M, Hatazawa J. Effect of aging on cerebral vascular response to Paco2 changes in humans as measured by positron emission tomography. J Cereb Blood Flow Metab 2002;22:997–1003. [PubMed: 12172385]

Janne d'Othee B, Rachmuth G, Munasinghe J, Lang EV. The effect of hyperoxygenation on T1 relaxation time in vitro. Acad Radiol 2003;10:854–860. [PubMed: 12945919]

Kato H, Yoshikawa T, Oku N, Imaizumi M, Takasawa M, Kimura Y, Kajimoto K, Tanaka M, Kitagawa K, Hori M, Hatazawa J. Statistical parametric analysis of cerebral blood flow in vascular dementia with small-vessel disease using tc-HMPAO SPECT. Cerebrovasc Dis 2008;26:556–562. [PubMed: 18836267]Epub 2008 Oct 6

Kawamura J, Terayama Y, Takashima S, Obara K, Pavol MA, Meyer JS, Mortel KF, Weathers S. Leuko-araiosis and cerebral perfusion in normal aging. Exp Aging Res 1993;19:225–240. [PubMed: 8223824]

Kelley BJ, Petersen RC. Alzheimer's disease and mild cognitive impairment. Neurol Clin 2007;25:577–609. [PubMed: 17659182]

Kim SG. Quantification of relative cerebral blood flow change by flow-sensitive alternating inversion recovery (FAIR) technique: Application to functional mapping. Magn Reson Med 1995;34:293–301. [PubMed: 7500865]

Krejza J, Mariak Z, Walecki J, Szydlik P, Lewko J, Ustymowicz A. Transcranial color doppler sonography of basal cerebral arteries in 182 healthy subjects: Age and sex variability and normal reference values for blood flow parameters. AJR Am J Roentgenol 1999;172:213–218. [PubMed: 9888770]

LaSarge, CL.; Nicolle, MM. Comparison of different cognitive rat models of human aging. In: Bizon, JL.; Wood, AG., editors. Animal models of human cognitive aging. New York: Humana Press; 2009. p. 73-102.

Levy-Cooperman N, Burhan AM, Rafi-Tari S, Kusano M, Ramirez J, Caldwell C, Black SE. Frontal lobe hypoperfusion and depressive symptoms in alzheimer disease. J Psychiatry Neurosci 2008;33:218–226. [PubMed: 18592038]

Lu H, Donahue MJ, van Zijl PC. Detrimental effects of BOLD signal in arterial spin labeling fMRI at high field strength. Magn Reson Med 2006;56:546–552. [PubMed: 16894581]

Lu J, Dai G, Egi Y, Huang S, Kwon SJ, Lo EH, Kim YR. Characterization of cerebrovascular responses to hyperoxia and hypercapnia using MRI in rat. Neuroimage 2009;45:1126–1134. [PubMed: 19118633]Epub 2008 Dec 14

Martin AJ, Friston KJ, Colebatch JG, Frackowiak RS. Decreases in regional cerebral blood flow with normal aging. J Cereb Blood Flow Metab 1991;11:684–689. [PubMed: 2050757]

Moeller JR, Ishikawa T, Dhawan V, Spetsieris P, Mandel F, Alexander GE, Grady C, Pietrini P, Eidelberg D. The metabolic topography of normal aging. J Cereb Blood Flow Metab 1996;16:385–398. [PubMed: 8621743]

Pagani M, Salmaso D, Jonsson C, Hatherly R, Jacobsson H, Larsson SA, Wagner A. Regional cerebral blood flow as assessed by principal component analysis and (99m)tc-HMPAO SPET in healthy subjects at rest: Normal distribution and effect of age and gender. Eur J Nucl Med Mol Imaging 2002;29:67–75. [PubMed: 11807609]Epub 2001 Nov 14

Paxinos, G.; Watson, C. The rat brain in stereotaxic coordinates. Burlington, MA: Academic Press; 2007.

SAS Institute Inc.. Logistic regression examples using the SAS system. Cary: SAS Insitute, Inc.; 1995. p. 163

Schultz SK, O'Leary DS, Boles Ponto LL, Watkins GL, Hichwa RD, Andreasen NC. Age-related changes in regional cerebral blood flow among young to mid-life adults. Neuroreport 1999;10:2493–2496. [PubMed: 10574358]

Sicard K, Shen Q, Brevard ME, Sullivan R, Ferris CF, King JA, Duong TQ. Regional cerebral blood flow and BOLD responses in conscious and anesthetized rats under basal and hypercapnic conditions: Implications for functional MRI studies. J Cereb Blood Flow Metab 2003;23:472–481. [PubMed: 12679724]

Sicard KM, Duong TQ. Effects of hypoxia, hyperoxia, and hypercapnia on baseline and stimulus-evoked BOLD, CBF, and CMRO2 in spontaneously breathing animals. Neuroimage 2005;25:850–858. [PubMed: 15808985]

Sonntag WE, Lynch CD, Cooney PT, Hutchins PM. Decreases in cerebral microvasculature with age are associated with the decline in growth hormone and insulin-like growth factor 1. Endocrinology 1997;138:3515–3520. [PubMed: 9231806]

Takahashi H, Kirsch JR, Okada T, Traystman RJ. Intensity of halothane- and hypercapnia-induced cerebral hyperemia is strain-dependent in rats. Anesth Analg 1996;83:359–365. [PubMed: 8694319]

Wang H, Golob E, Bert A, Nie K, Chu Y, Dick MB, Mandelkern M, Su MY. Alterations in regional brain volume and individual MRI-guided perfusion in normal control, stable mild cognitive impairment, and MCI-AD converter. J Geriatr Psychiatry Neurol 2009;22:35–45. [PubMed: 19150973]Epub 2009 Jan 15

Zaharchuk G, Martin AJ, Rosenthal G, Manley GT, Dillon WP. Measurement of cerebrospinal fluid oxygen partial pressure in humans using MRI. Magn Reson Med 2005;54:113–121. [PubMed: 15968660]

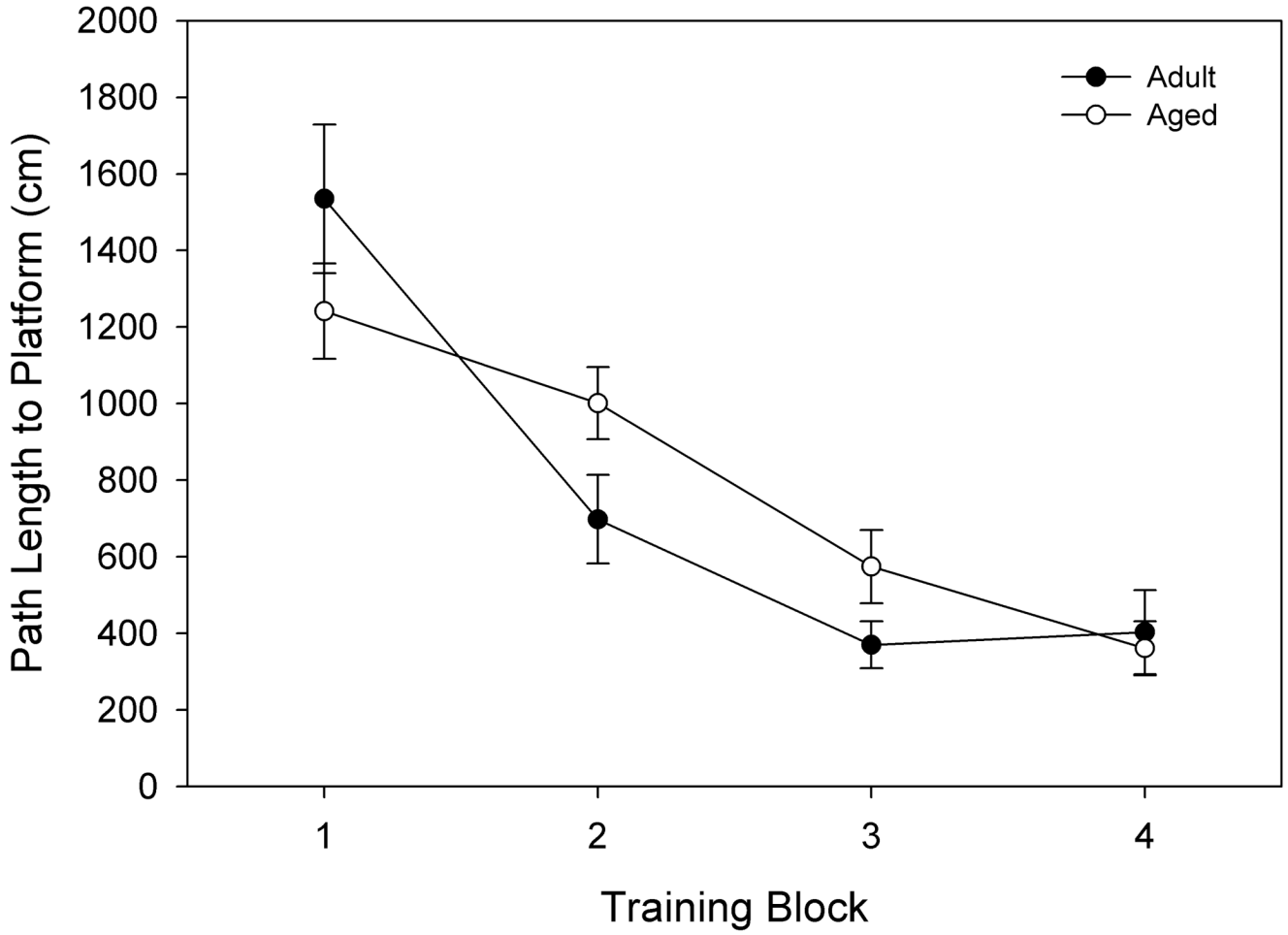

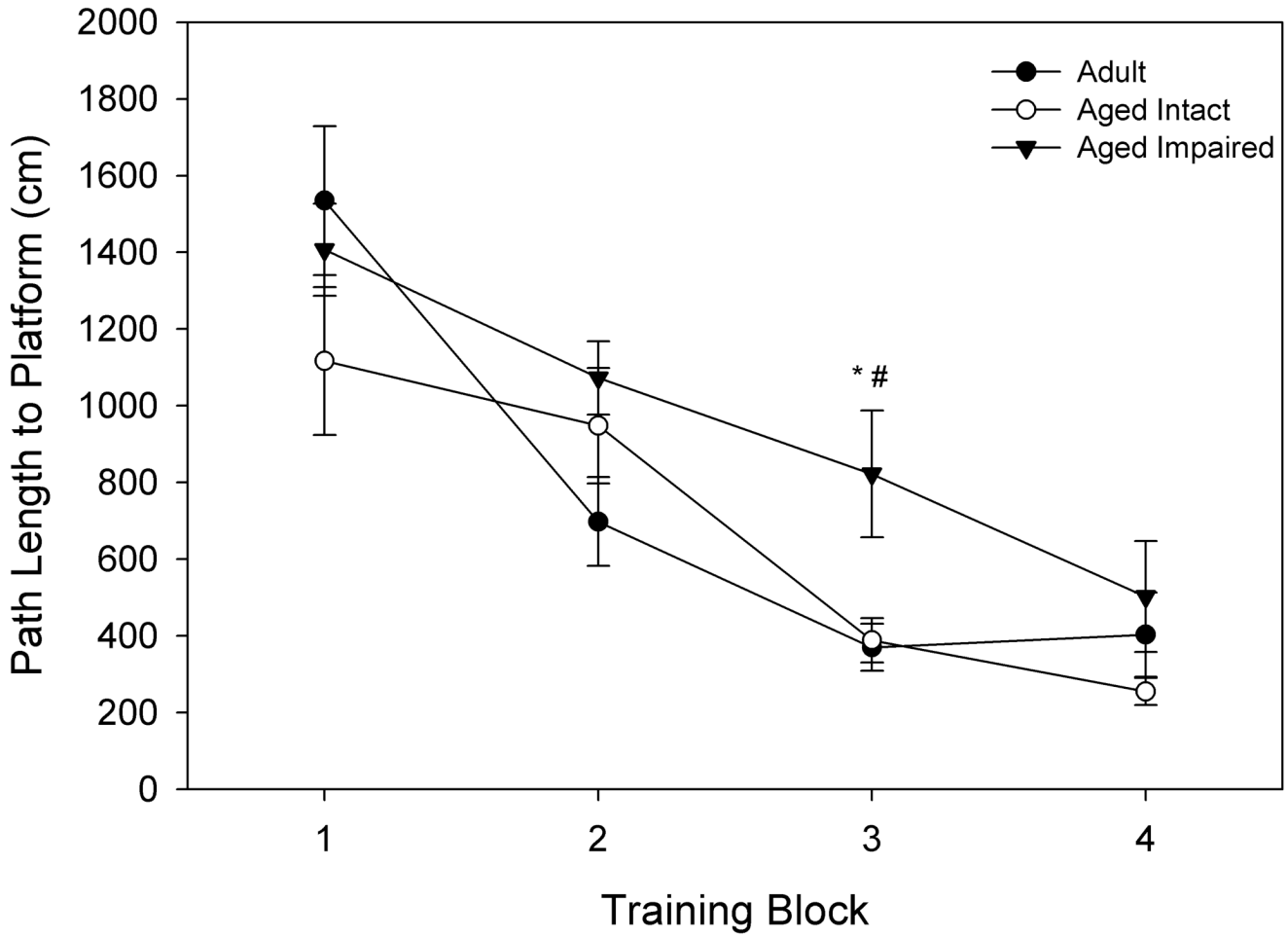

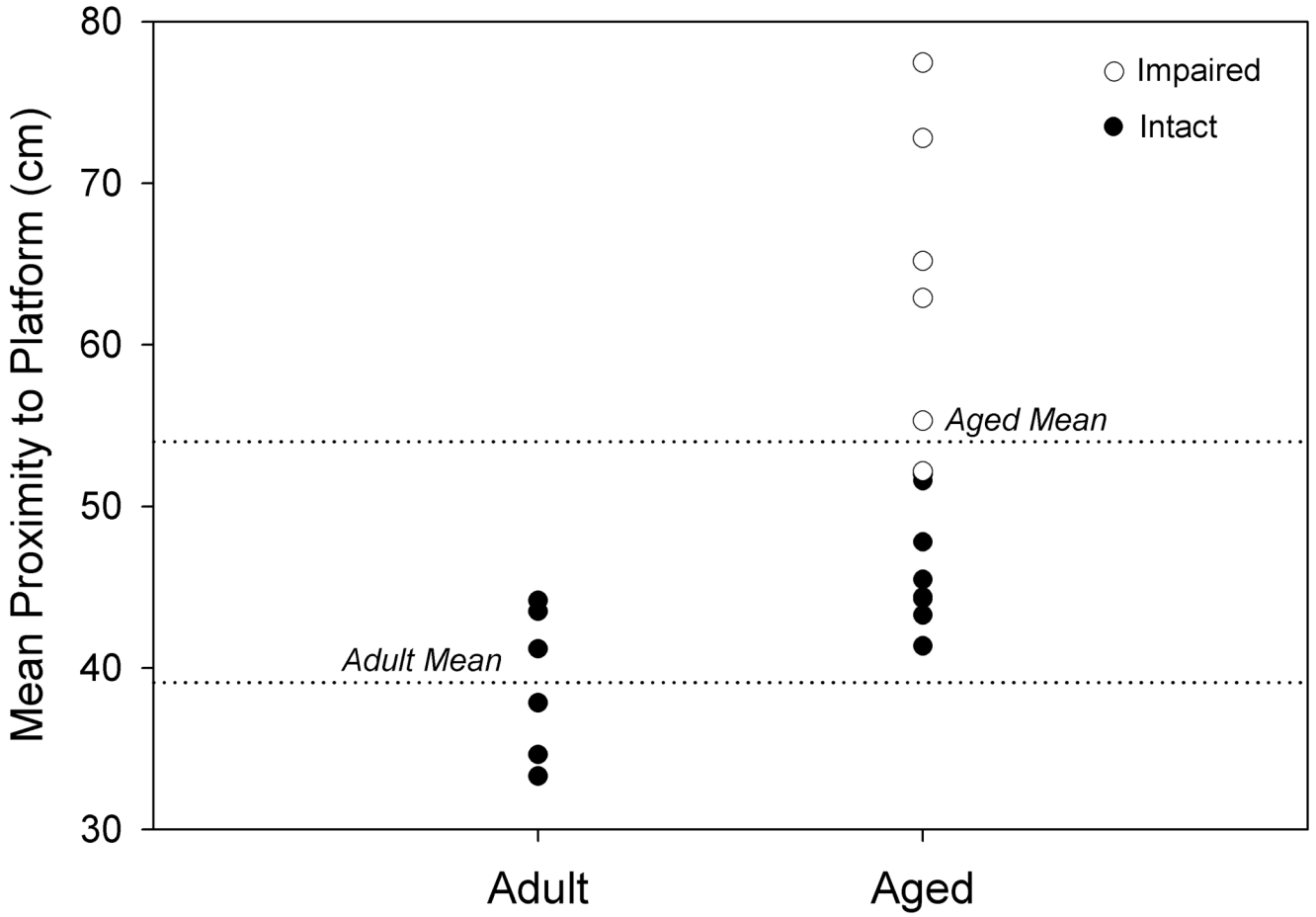

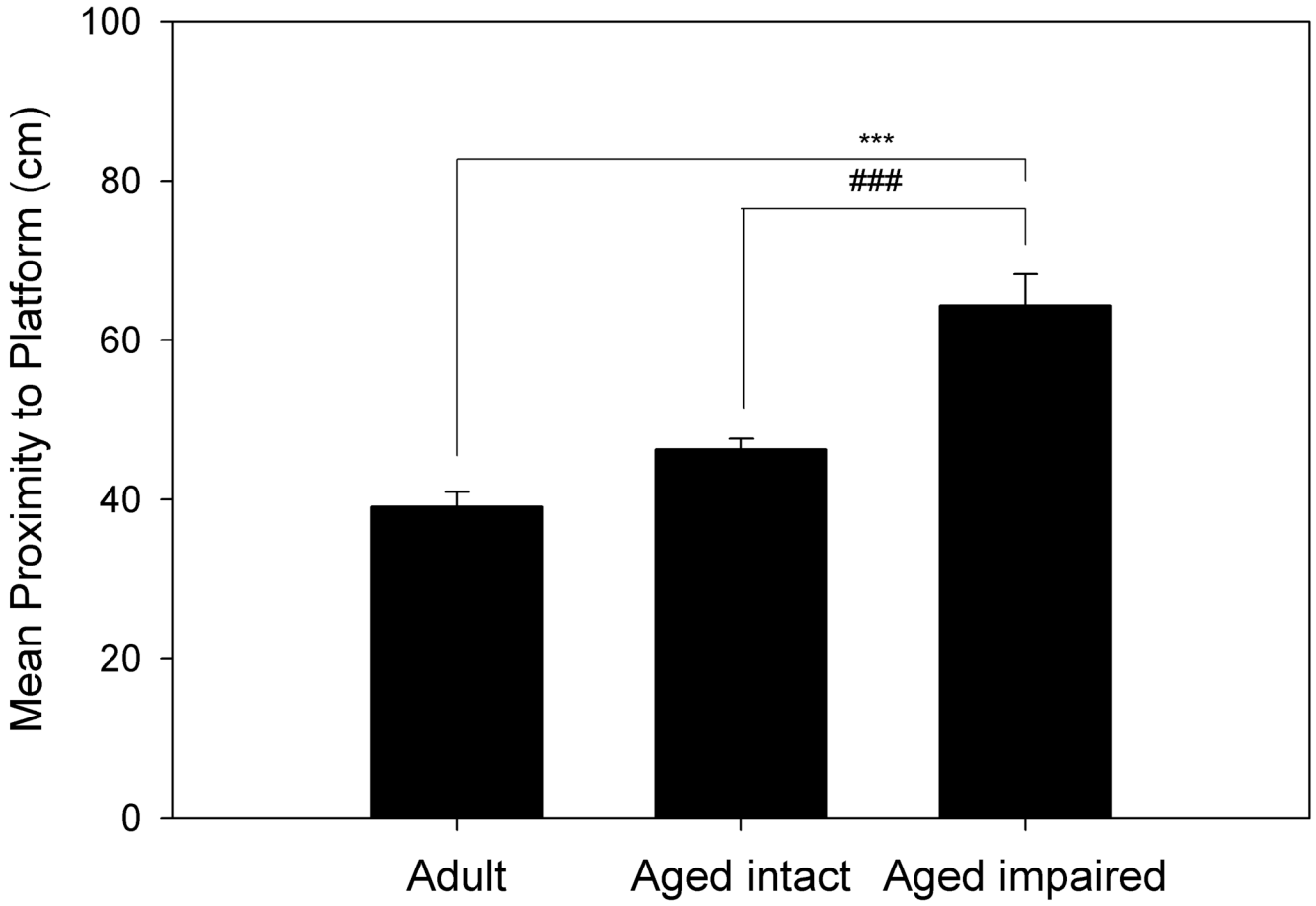

Figure 1. Separation of animals by spatial memory performance

Hippocampally-dependent tests of learning and memory were conducted in a Morris Water Maze. Animals were permitted 3 trials/day for 8 days and every 6th trial included a 30s probe trial when the escape platform was unavailable. Data shown for *A.* and *B.* are path length before finding the platform in training trials, and data for *C.* and *D.* are mean proximity to the platform for the final 3 probe trials. ***A.*** Acquisition of spatial memory, as measured by the length of the path used to search for the platform during training trials of aged and adult animals. Both age groups were capable of learning the task, but there was a significant effect of age across all blocks (p= 0.037). ***B.*** Acquisition of spatial memory for animals classified (as in *C.*) by memory performance. Animals classified as impaired by the proximity measure were the primary contributors to the age difference seen in *A.* ***C.*** Using probe trial data, aged animals (n= 14) were divided into intact and impaired groups as described in the text, 2.86 standard deviations above the mean score for adult animals (n= 6). ***D.*** Separation of the aged animals based on this measure resulted in an aged intact group with probe trial performance not significantly different from adult animals, while performance of aged impaired animals was significantly different from aged intact and adult animals. * p= 0.022 compared to adult animals, # p= 0.018 compared to aged intact animals, *** p< 0.001 compared to adult animals, ### p< 0.001 compared to aged intact animals.

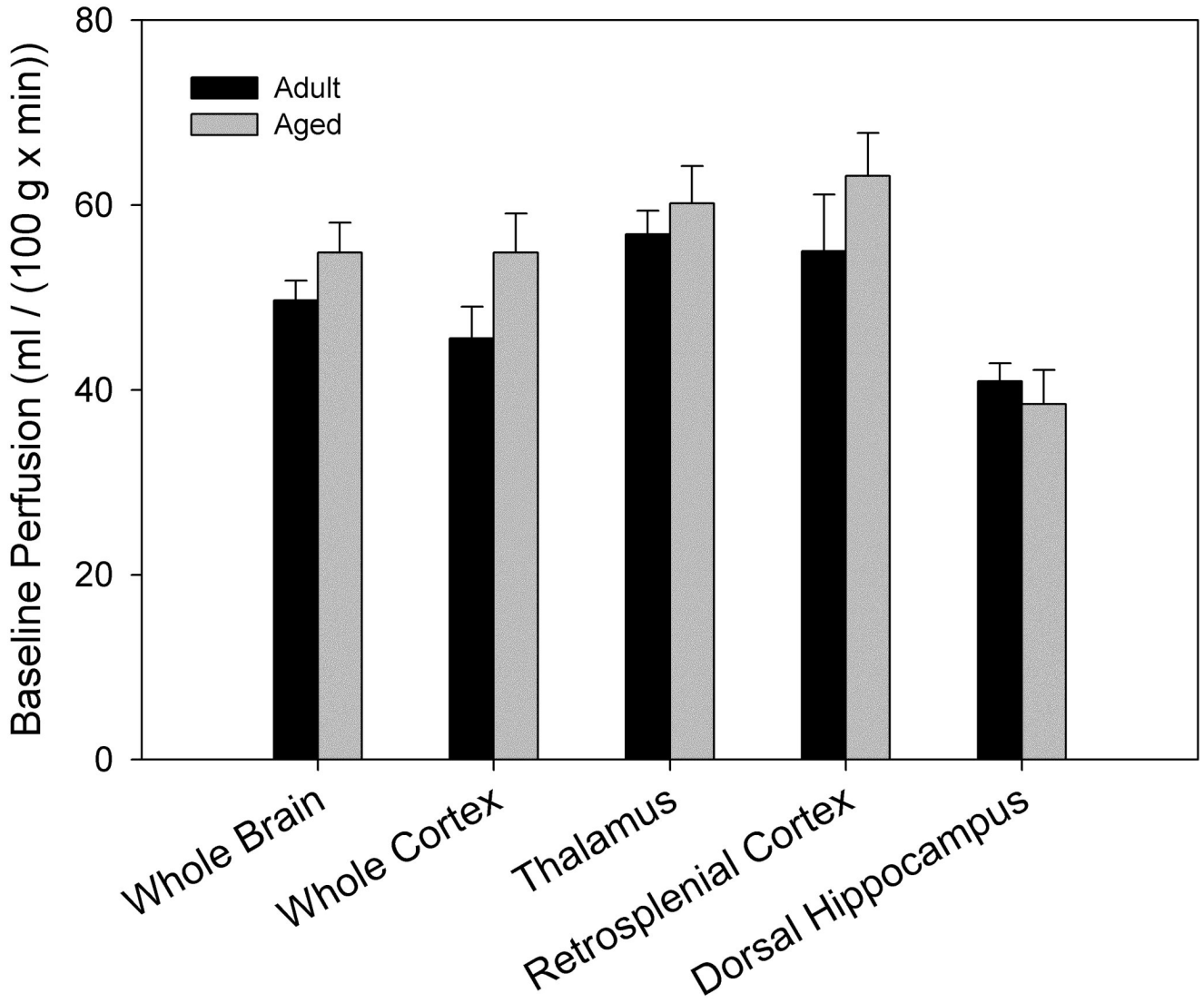

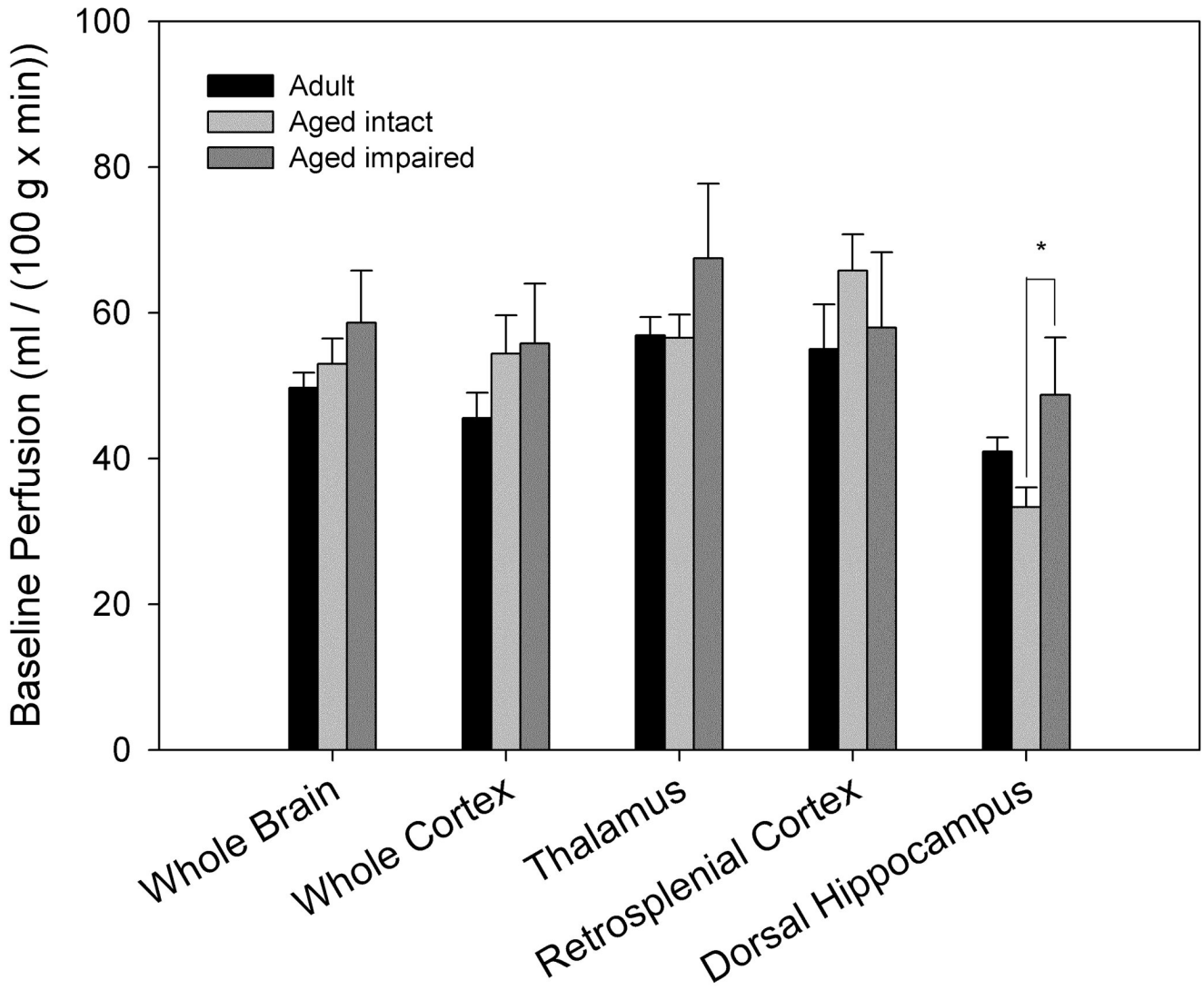

Figure 2. Basal cerebrovascular perfusion differs by spatial memory performance

High resolution images using a rapid acquisition, relaxation-enhanced (RARE) pulse sequence were acquired for morphologic reference purposes. Regions of interest were manually outlined and included the entire cross-section of the brain, cortex, dorsal hippocampus, retrosplenial cortex and the thalamus. For FAIR analysis, the recovery curves obtained from each pixel of the global or selective inversion images were numerically fitted to an exponential model and longitudinal recovery rates were then used to calculate the perfusion rate, f (ml/(100g × min)) on a pixelwise basis using the relationship $f = \lambda \cdot (1/\tau_{NS} - 1/\tau_{SS})$. Areas overlapping large blood vessels or ventricles were removed. ***A.*** No significant differences in basal perfusion were found between age-groups (n_{adult}= 6, n_{aged}= 12). ***B.*** Separation of aged animals by maze performance revealed significantly higher perfusion of dorsal hippocampus in aged impaired (n= 4) when compared to aged intact (n= 8) animals (p= 0.045).

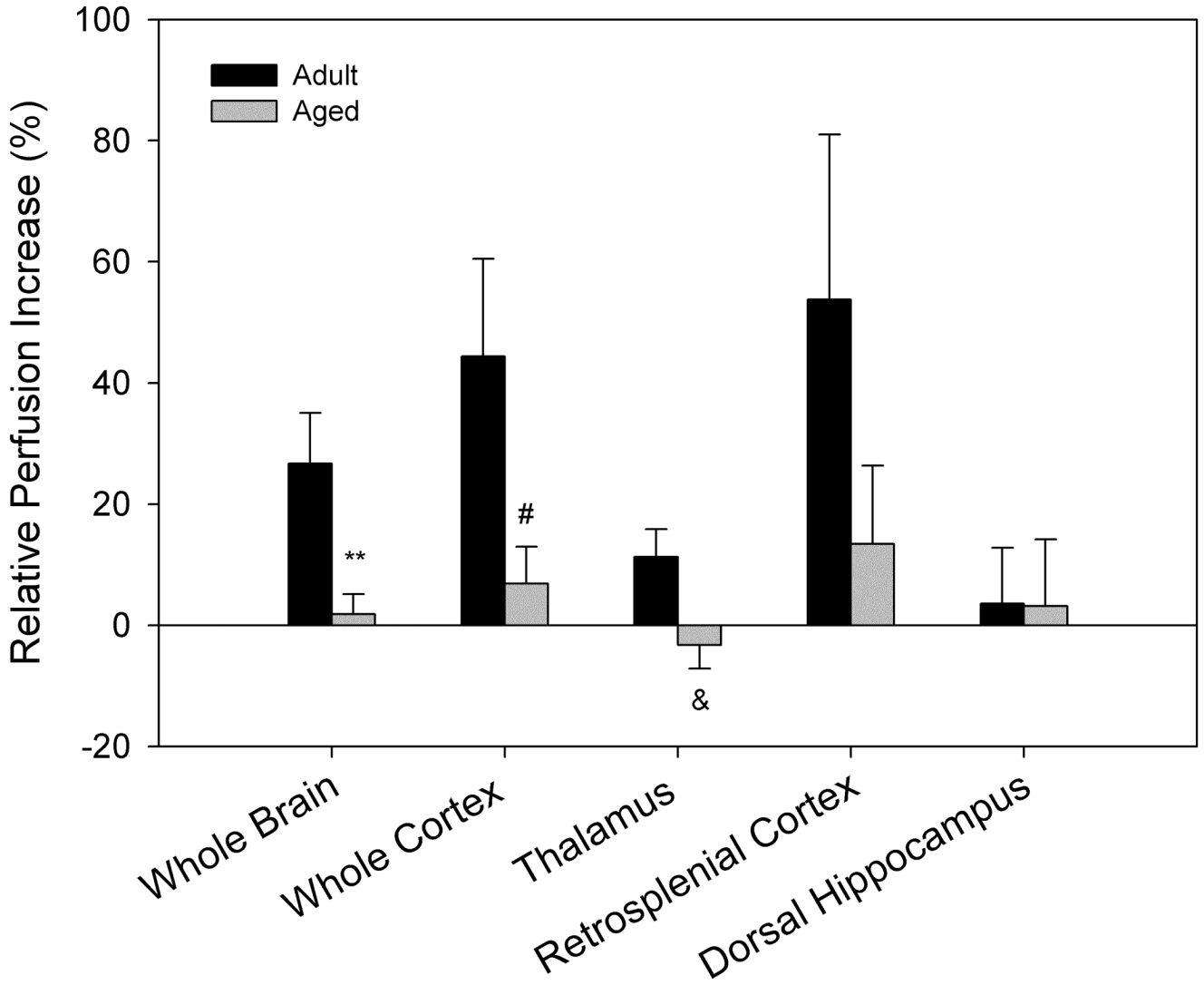

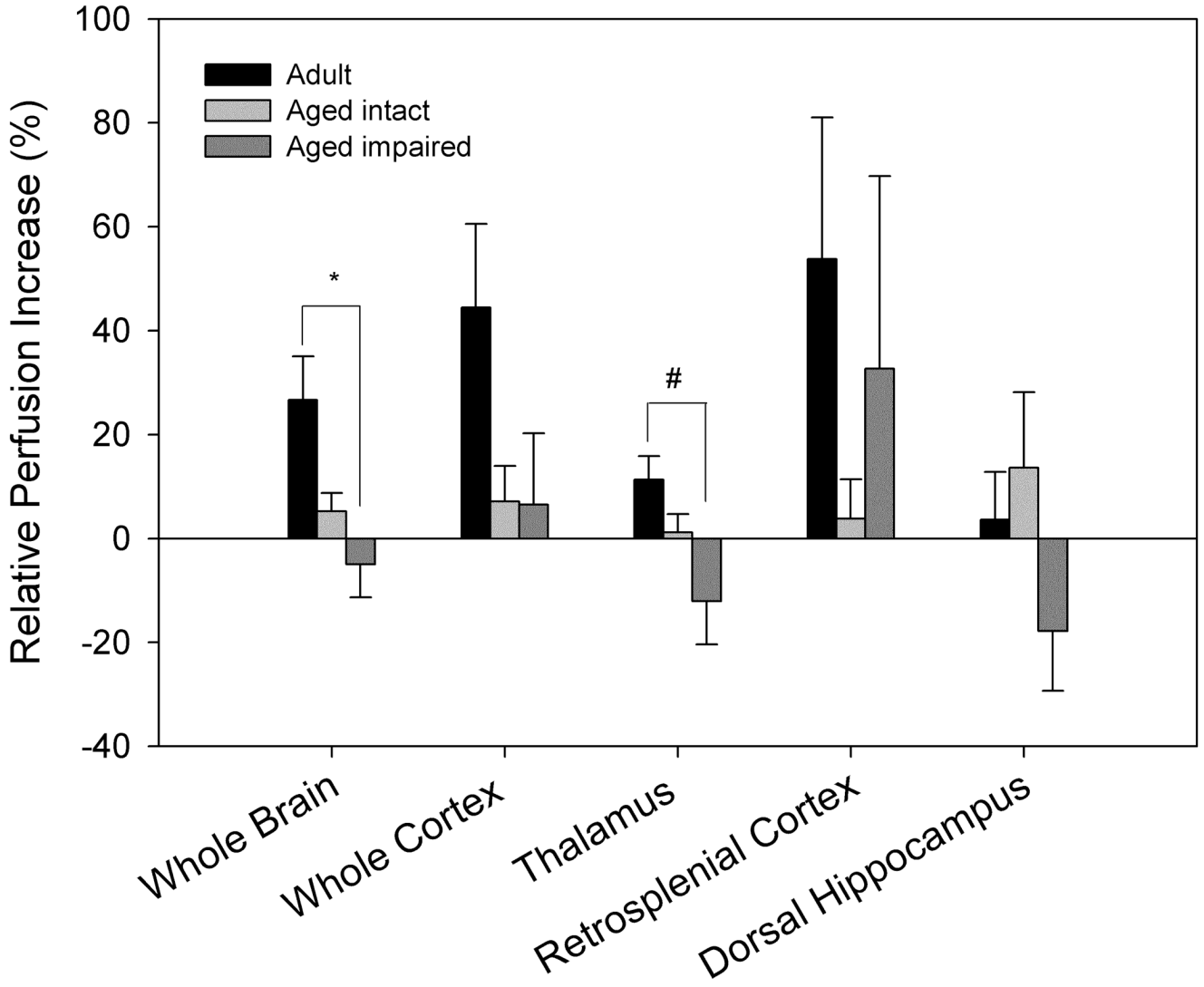

Figure 3. FAIR analysis indicates that perfusion response to hypercapnia differs by age and performance

A. Aged animals (n= 12) show diminished response to 10% CO_2 compared to adult animals (n= 6) across the entire brain section, cortex, and thalamus (**p= 0.004, #p= 0.017, &p= 0.036 compared to adult animals). ***B.*** Separation of aged animals by performance demonstrates significant differences between aged impaired (n= 4) and adult animals (n= 6) in whole brain and thalamic perfusion response to hypercapnia (*p= 0.014, #p= 0.025), while no significant differences between aged intact (n= 8) and adult animals were evident.

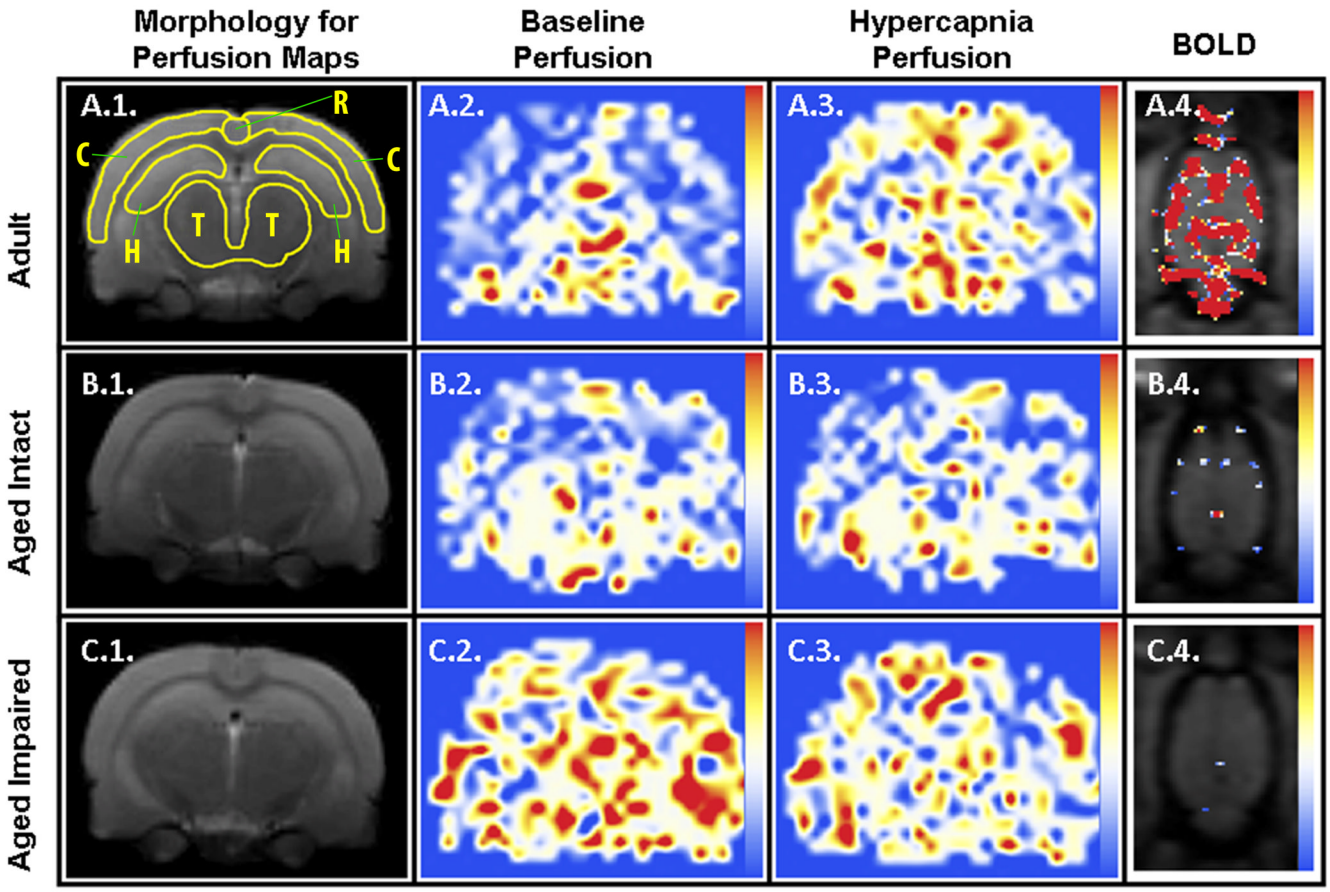

Figure 4. Representative MR-derived parametric maps

Coronally-oriented perfusion maps of adult (row A), aged intact (row B), and aged impaired (row C) animals before (column 2) and during (column 3) hypercapnia are linearly color-coded from 0 (blue) to 150 (red) ml / (100g × min) using the color scale shown on the right, and cropped to final dimensions of 9.1mm×11.6mm. Corresponding morphologic RARE reference images are shown (column 1) along with the regions of interest used for analyses as yellow outlines (A.1.; C: whole cortex, T: thalamus, R: restrosplenial cortex, H: dorsal hippocampus). BOLD correlation maps (column 4) between the T2*-weighted signal and hypercapnia stimulation are represented using the linear color scale shown to the right, with correlation values ranging from 0.6 (blue) to 0.8 (red). The first T2* image of the series is used as a grayscale background for morphological reference. Here, only one of the 8 available horizontal slices is shown, cropped to final dimensions of 25mm×17.7mm. Statistical analysis (Fig. 5) was performed only on those pixels that intersect the FAIR coronal section of the brain.

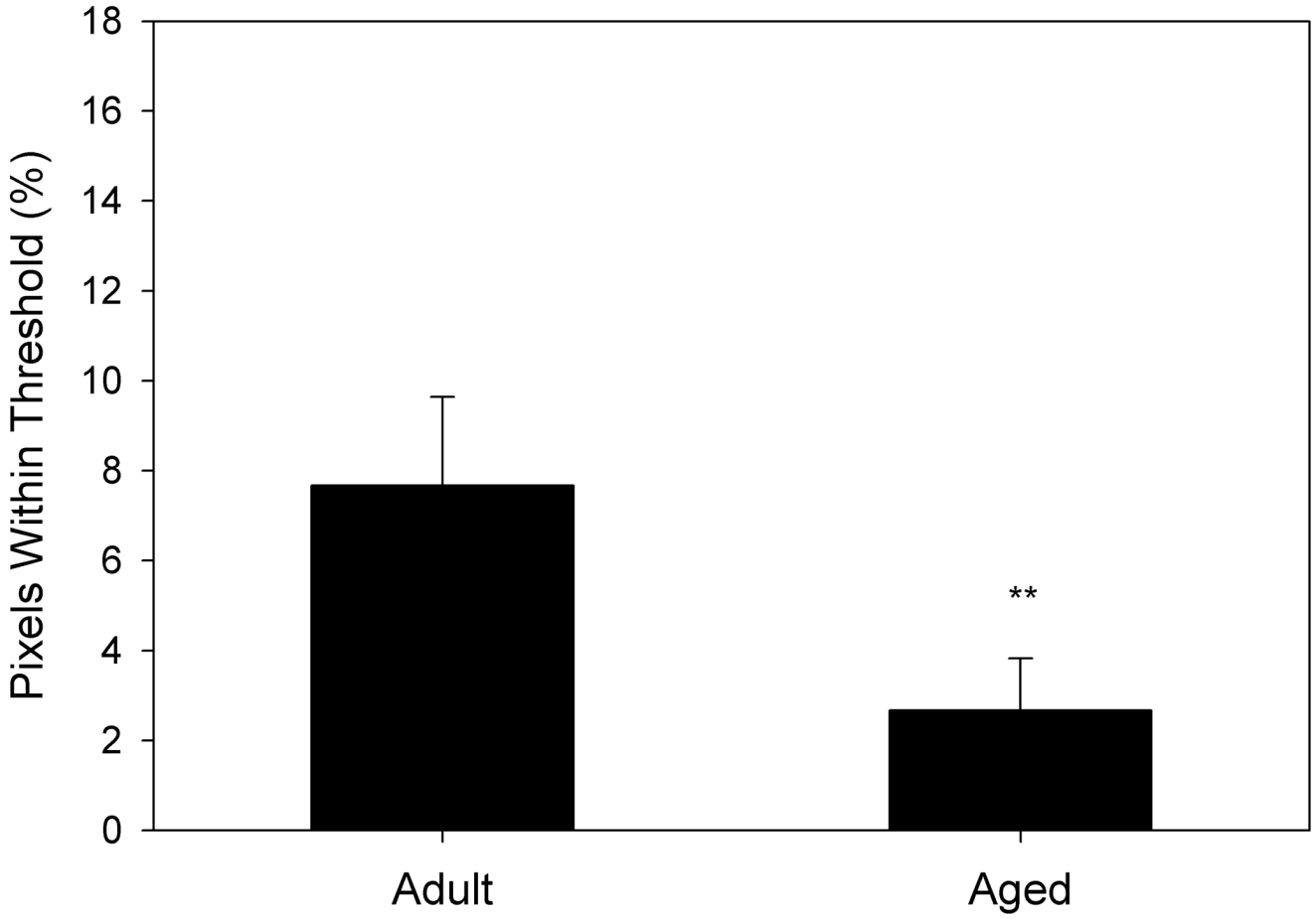

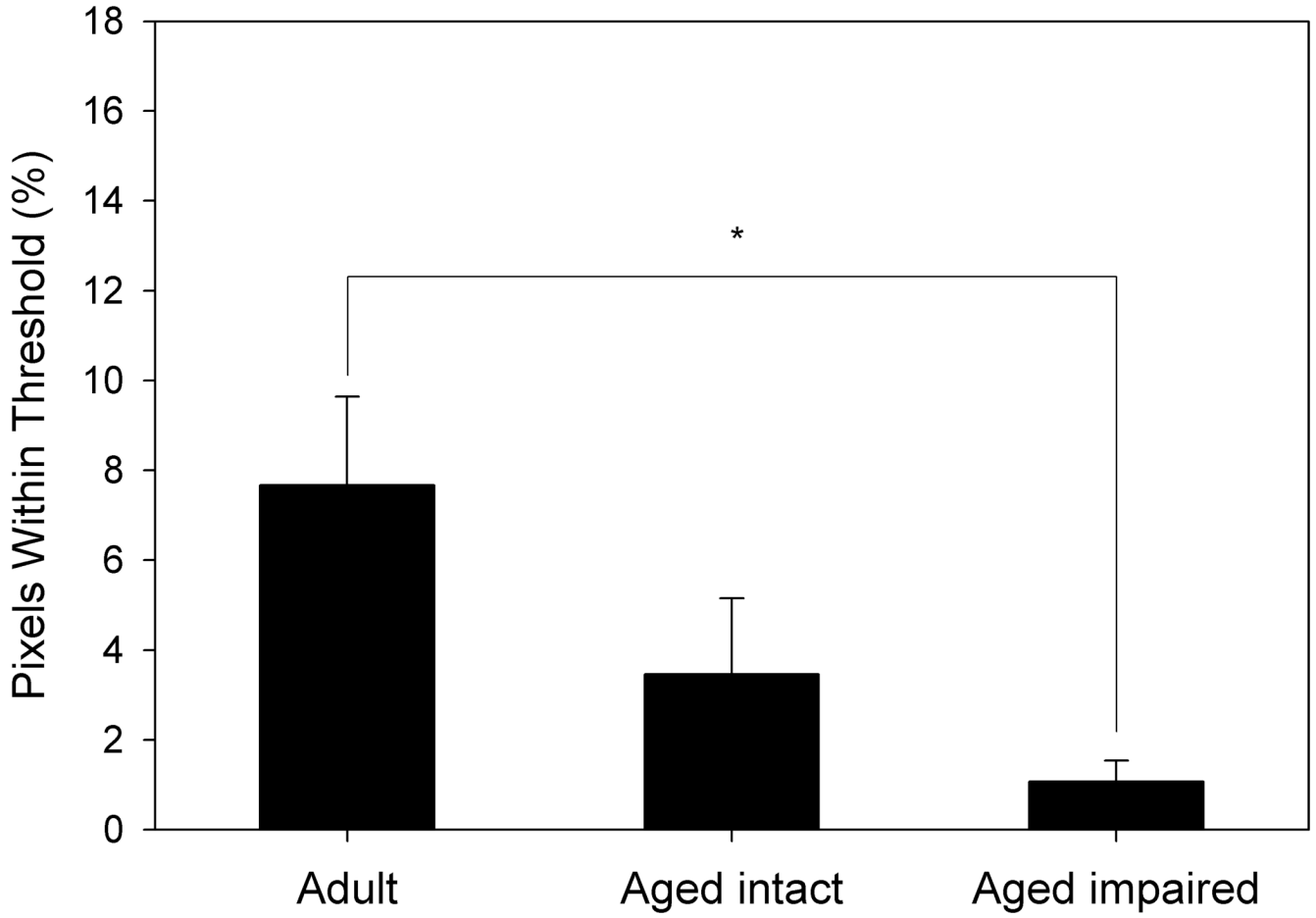

Figure 5. Response to hypercapnia measured by BOLD fMRI differs by age and performance

A. Aged animals (n= 12) demonstrate a markedly reduced response to hypercapnia compared to adult animals (n= 6). ***B.*** Aged impaired animals show a significant reduction in response to hypercapnia compared to adult animals, whereas differences between aged intact and adult animals are not statistically significant. *p= 0.03, **p= 0.004 compared to adult animals.

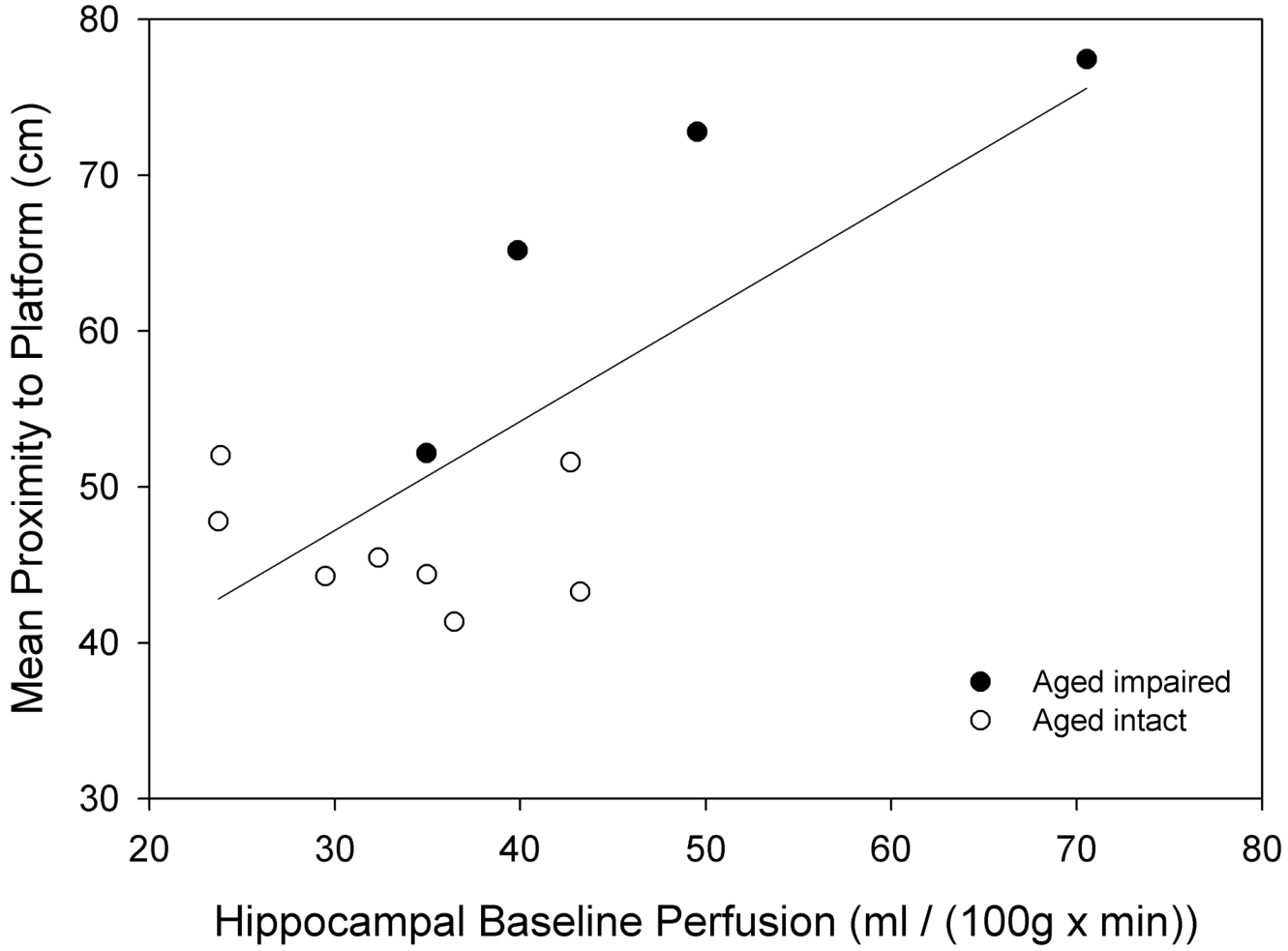

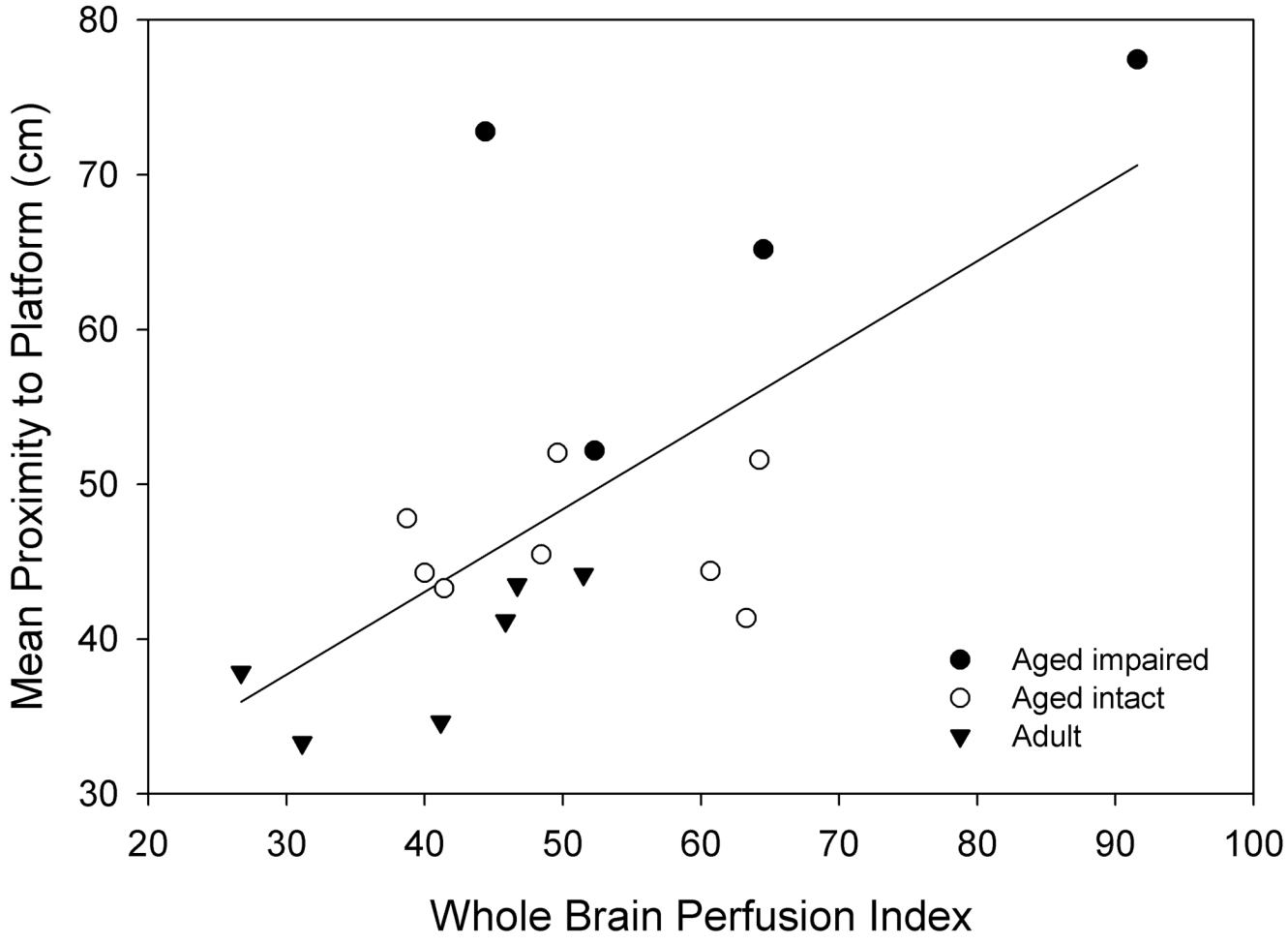

Figure 6. Perfusion measurements are predictive of spatial memory in linear regressions

A. Increased baseline perfusion of dorsal hippocampus is predictive of poorer spatial memory in aged animals (n= 12, r^2= 0.54, p= 0.006). ***B.*** A perfusion index, combining baseline and perfusion response to hypercapnia (see text) across the entire section, increases with diminished spatial memory across all groups (n= 18, r^2= 0.432, p= 0.003).

Table 1
Apparent Longitudinal Relaxation Rates in FAIR

Longitudinal relaxation rates are presented as defined in data processing. The rates obtained from slice-selective (SS) inversion images are systematically higher than those obtained from non-selective (NS) inversion images. In all cases, values are higher under hypercapnia than in the basal state.

	$R_{1,ns}$	$R_{1,ss}$	Significance
Adult, baseline	674.2 1.4	683.4 1.2	***
Adult, hypercapnia	707.8 3.6	719.3 3.6	*
Aged, baseline	678.9 3.2	689.0 3.3	*
Aged, hypercapnia	710.2 2.9	720.5 3.1	*

$n_{adult}= 6$, $n_{aged}= 12$

* $p< 0.05$

*** $p< 0.001$.